Supporting Information: Glycerol Prevents Dehydration in Lipid Cubic Phases

*Samuel J. Richardson, Paul A. Staniec, Gemma E. Newby, Johnathon L. Rawle, Adam R. Slaughter, Nick J. Terrill, Joanne M. Elliott, Adam M. Squires**

S1: Experimental Methods

All compounds were used as received. Phytantriol (3,7,11,15-tetramethyl-1,2,3-hexadecanetriol) was received as a gift from Adina Cosmetic Ingredients (UK). Rylo 19^{TM}, an industrial form of monoolein (2,3-dihydroxypropyl (Z)-octadec-9-enoate)[1], was received as a gift from Danisco (UK). Glycerol (propane-1,2,3-triol) was purchased from Sigma (UK).

Lipid (phytantriol or Rylo) / ethanol and glycerol / ethanol solutions were prepared at 80% (w/w) ethanol with heating at 50 °C to assist in dissolution. On cooling, the glycerol and lipid solutions were combined in different ratios to produce mixtures that were all 80% (w/w) ethanol, and which, following ethanol evaporation during spin-coating, had concentrations of (0%, 5%, 10%, 20%, 25%) glyocerol:phytantriol or (0%, 20%, 40%) (w/w) glycerol:Rylo respectively. Round silicon wafers (diameter = 2 cm) were made hydrophobic as described in our previous paper[2].

For the spin-coating, 100 µl of lipid/glycerol/ethanol solution was deposited onto wafers by spin coating at speeds of 1, 5 and 10 kRPM over 40 s. This was sufficient time for the ethanol to evaporate, by visual inspection (the films were colored, due to interference, and color changes were observed during ethanol evaporation). Ethanol (100 µl) was applied to the wafer edge during a second 30 s rotation at 5 kRPM in order to remove excess buildup of solution at the edges of the disc. Finally discs were left in air for half an hour before analysis. Once prepared, ellipsometry was used to measure the thickness of the films which varied between 550 nm and 1450 nm as shown in Figure S2.

GISAXS measurements were performed at beamline I07 at Diamond Light Source using a beam size of 300 µm x 500 µm with energy of 12.5 KeV. A Pilatus 100K detector was used to collect data over a q range of 0.01 $Å^{-1}$ to 0.50 $Å^{-1}$. A sample of silver behenate was used as a calibrant in order to measure the sample to detector distance and beam center. A vertical rod was used as a beamstop to block the direct and reflected beams.

The samples were contained within a controlled-humidity cell (183mm diameter, ~2.5 L) with polyimide walls to allow for X-ray transmission. The RH was controlled over a range of 10 % to 97 % using a combination of hydrating sources (water-soaked tissue paper and/or pipe cleaners) and a variable dry helium line-in; a handheld Vaisala HM70 humidity sensor (factory calibration, ± 0.6 RH at 0 – 40 % RH and ± 1 RH at 40 – 97 % RH) was placed near the sample in the chamber to monitor humidity. GISAXS images of 1 s exposure were taken regularly as the humidity of the sample environment was varied.

Two- dimensional GISAXS images were radially integrated over one quadrant using YAXS[3], a custom macro that runs within the ImageJ software package. Phases were identified by assigning peaks measured to Bragg reflections for a given phase.

S2: Film thickness

A Brewster Angle Microscope spectroscopic ellipsometer was used to estimate the thickness of lipid/glycerol films at ambient humidity (approx. RH = 50 %). Measurements of the angles Delta (Δ, the phase shift between incident and reflected beam) and Psi (ψ, the amplitude ratio between the p and s polarized waves in the reflected beam) were performed with the angle of incidence set to 75° over the wavelengths 350 – 1000 nm. 'ELLIPSHEET '[4] was used to simulate ψ and Δ where film thickness was found by minimizing the sum of the squares of the deviations between the simulated and measured data. For air n=1 and k =0; for phytantriol/glycerol films the refractive index was assumed to be n = 1.47[5,6] and k is also equal to zero. Silicon has a non-zero extinction coefficient and a complex refractive index which varies over wavelengths; at λ=360nm n =6.01 and k=2.91 and at λ=1000nm n=3.57 and k=0.00[7].

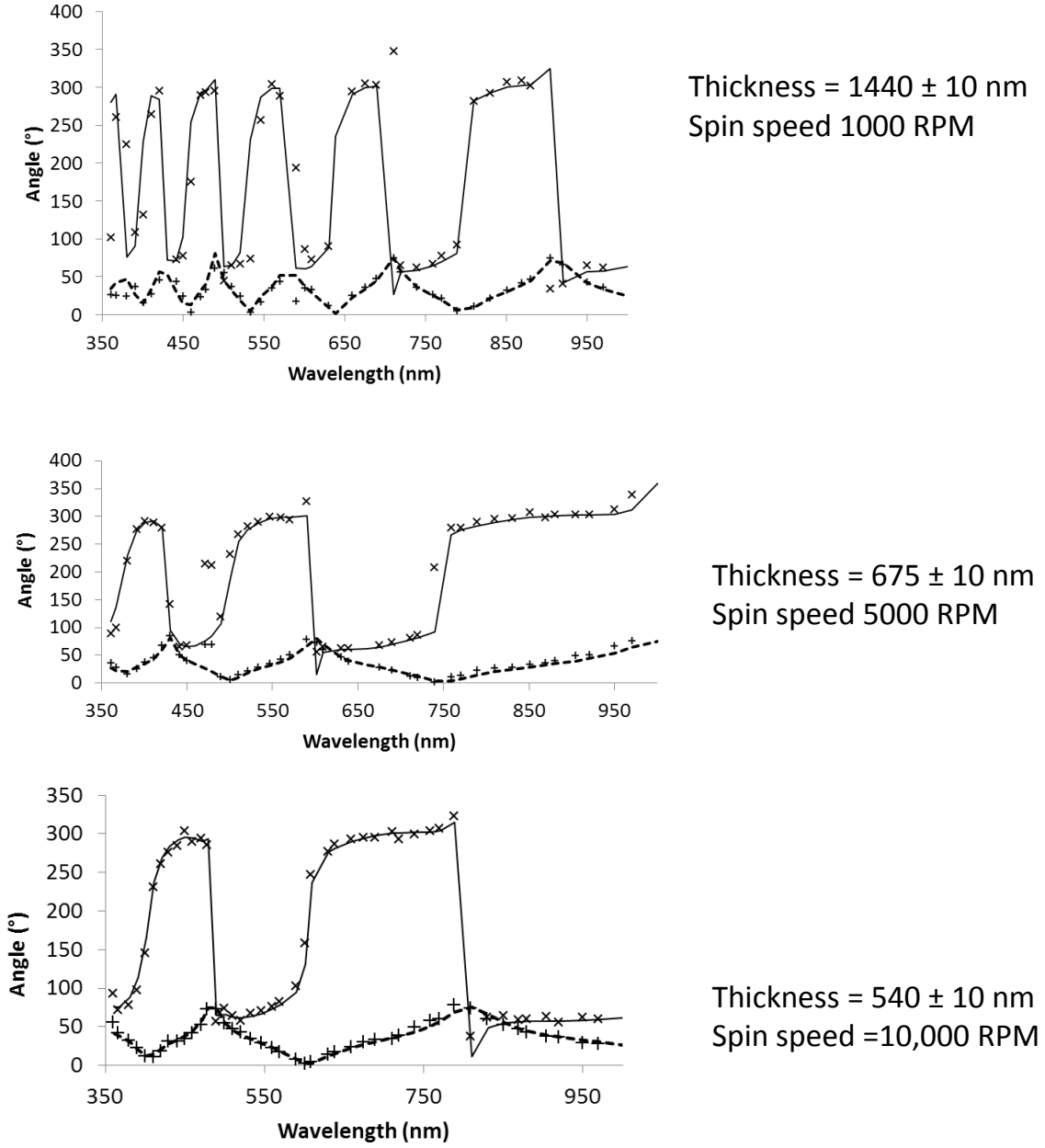

Figure S2. Ellipsometric data from films prepared by spin-coating at three different speeds, producing films of different thickness. Solid and dotted lines represent simulated data, and × and + experimental data, for Δ and ψ respectively. All films were spun from a solution that was 80 wt % ethanol (20% phytantriol / glycerol). Top and bottom films were 20%:80% (w/w) glycerol:phytantriol, while the middle film was 5%:95% (w/w) glycerol:phytantriol.

S3: Phase Identification for phytantriol/glycerol films

Locations of the Q_{II}^{D}, Q_{II}^{G} and L_{II} phases with respect to RH were determined from characteristic Bragg peaks observed in 1D stacked plots shown in figure S2A. The location of the L_{α} phase was determined from the 2D images shown in figure S2B.

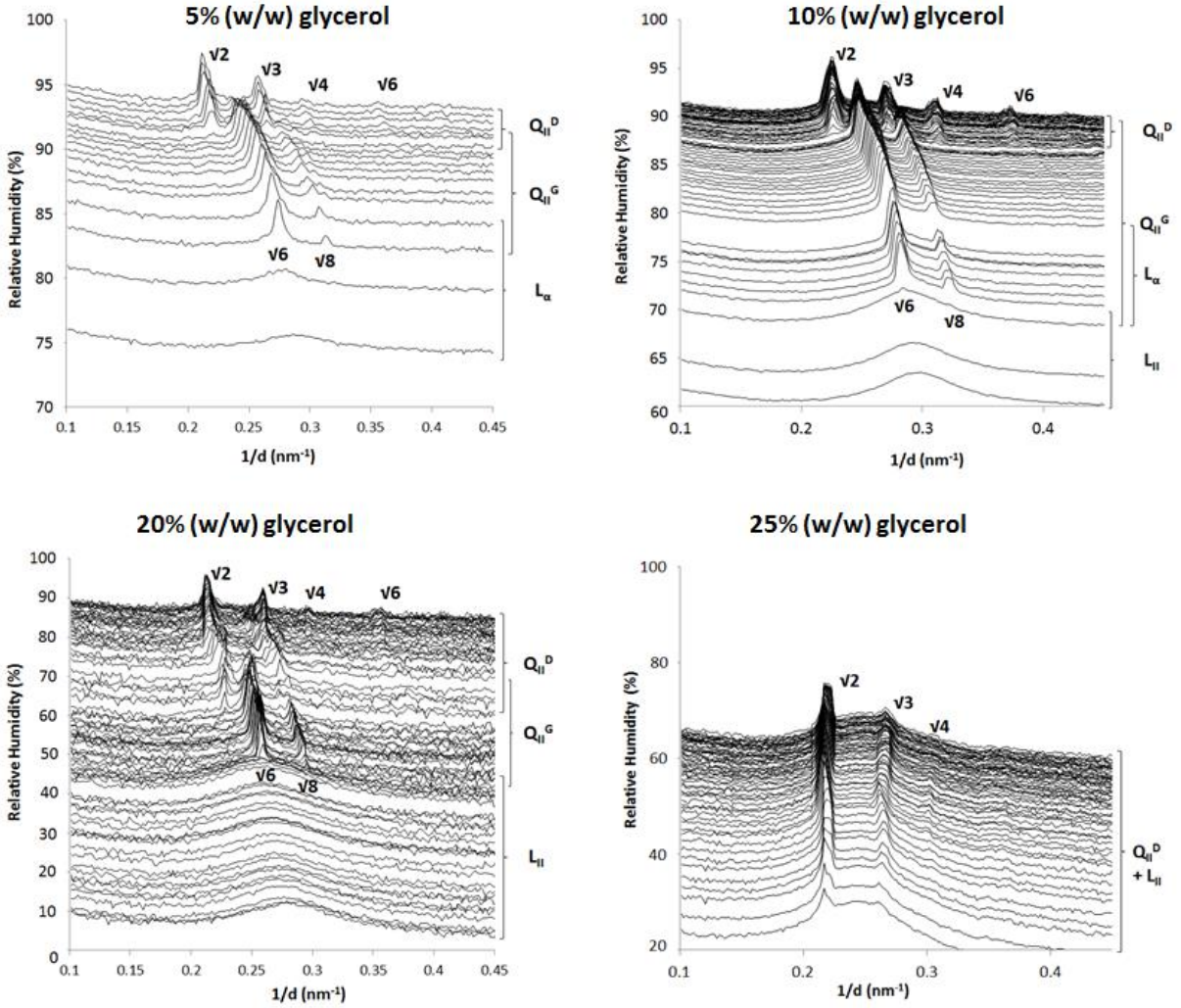

Figure S3A. Stacked GISAXS intensity profiles for thin films of phytantriol and 5%, 10%, 20% and 25% (w/w) glycerol taken as humidity was increased and plotted on a log scale. Phase locations and corresponding Bragg peaks are noted on each plot. The location of the L_{α} phase was deducted from figure S3B.

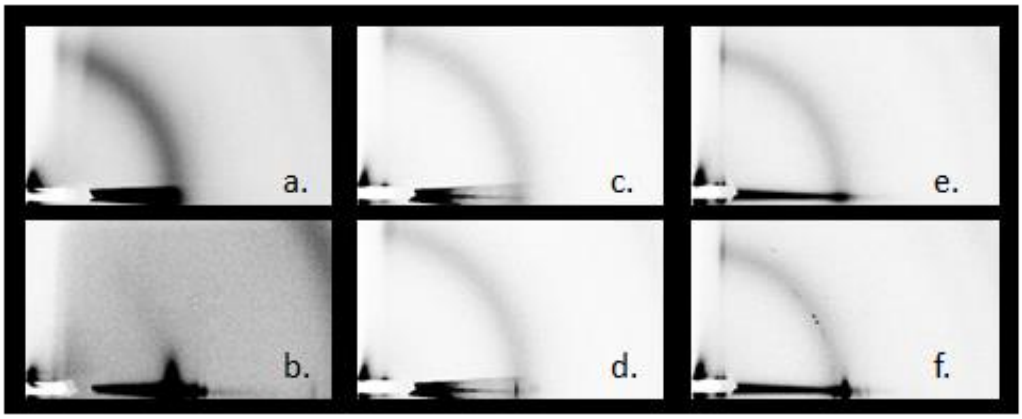

Figure S3B. 2D GISAXS images showing appearance of the L_α phase. (a)-(b) show images of phytantriol film with no added glycerol where the L_{II} phase is observed at RH = 92.8% (a) and the L_α phase forms at RH = 95.9 % (b). Images (c)-(d) show a film of phytantriol with 5% (w/w) glycerol where initially the L_{II} is observed at 82.7% (c) and at RH = 83.8% a coexistence of L_α and L_{II} can be observed (d). Images (e)-(f) show a film of phytantriol with 5% (w/w) glycerol where the L_{II} phase is observed at RH = 65.8 (e), the L_α phase is observed to appear at RH = 70% (f).

S4: Measurement of bulk phytantriol/glycerol samples

In order to estimate the phase that a film of phytantriol and glycerol would form at RH = 0% bulk samples of phytantriol/glycerol solution sealed in glass capillaries were measured using SAXS. Phytantriol and glycerol were first melted at 60 °C in order to ease measurement. Once correct concentrations were made samples were melted again and the shaken by hand in order to mix as samples returned to room temperature. Phytantriol/glycerol mixtures were poured into glass capillaries and sealed. SAXS measurements of both samples showed a broad ring indicating that both 5% and 10% (w/w) glycerol and phytantriol samples had formed the L_{II} phase.

SI5: Phytantriol and 5% (w/w) glycerol

Two samples were measured with 5% glycerol and phytantriol, labelled wafer 1 and wafer 4. Table S1 lists the observed phase locations. Wafer 1 maintained a L_α phase to the maximum measured humidity of RH = 94% with no Q_{II} phases observed. This suggests that the lower humidity limits for the two Q_{II} phases were above this, higher than those measured in wafer 4. Because no actual value can be associated with these transitions we could not meaningfully take an average of the values for wafers 1 and 4, and therefore only presented the values of 84% and 92.5% for wafer 4 in table 1. This is despite the fact that the average of the two values would have been significantly higher and would have given a better theoretical fit to the trend line in Figure 4.

Table S5. Observed phase locations with respect to relative humidity for two samples of phytantriol with 5% glycerol.

Wafer	L_{II} RH (%)	L_α RH (%)	Q_{II}^G RH (%)	Q_{II}^D RH (%)
1	71.0* - 91.3	73.0 – 94.1*	-	-
4	-	76.0* - 86.0	84.0 – 94.0	92.5 – 96.0*

* indicates where the maximum/minimum level of humidity measured is reached.

S6: Phase identification for Rylo/glycerol films

Q_{II} phase locations were determined from stacked scattering patterns by assigning peaks to Bragg peaks shown.

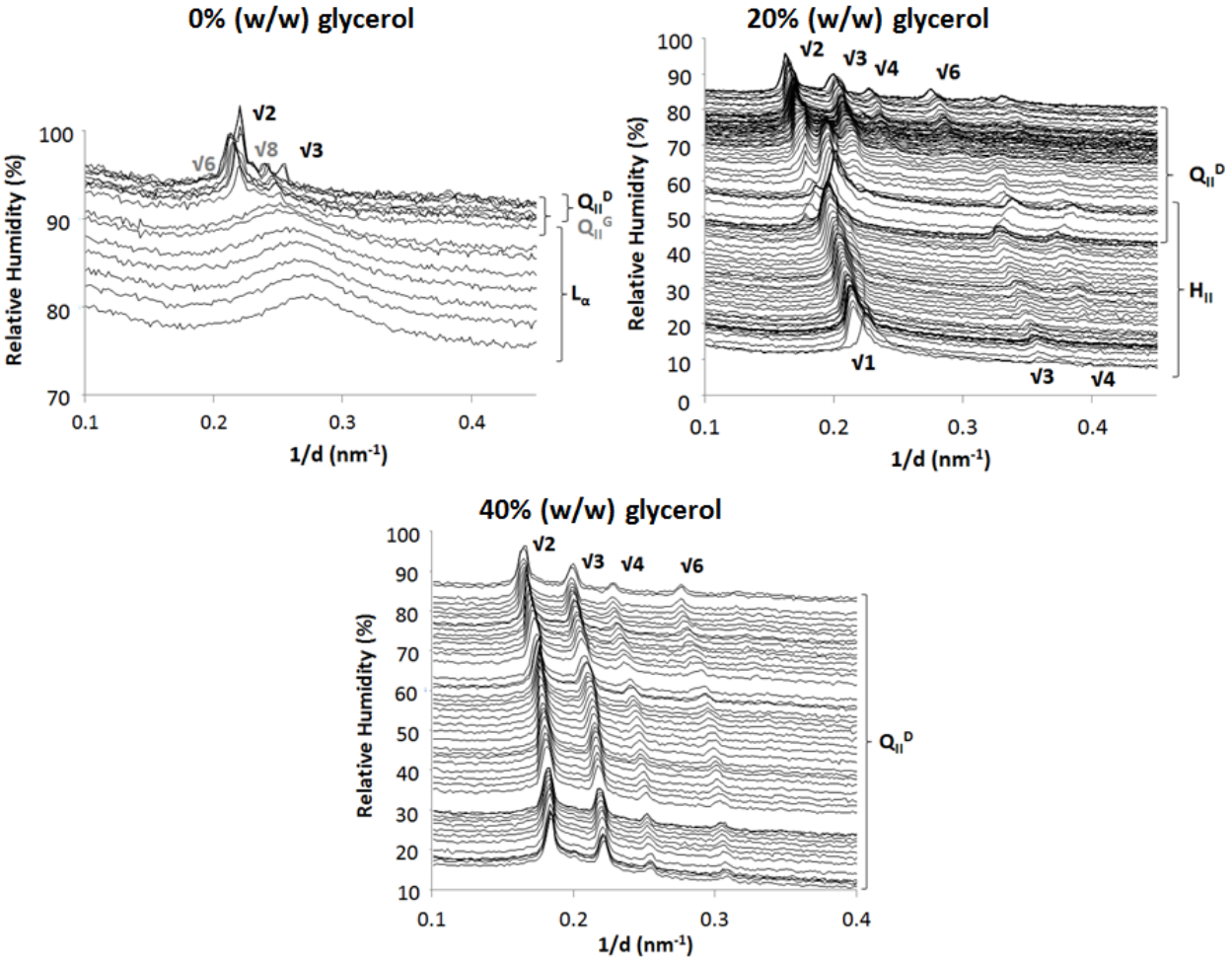

Figure S6. Stacked GISAXS intensity profiles for a thin film of Rylo with 0%, 20% and 40% (w/w) glycerol under increasing levels of humidity plotted on a log scale. Mesophases with corresponding Bragg peaks are notated on the plot.

Curiously, the 20% glycerol data indicate the presence of an inverse hexagonal phase at lower %RH values. This was not seen in any other sample, and as only one data set was obtained for this sample, we cannot say whether it is reproducible. We had considered the possibility that it is an artefact induced by beam damage; however, as it disappears on increasing humidity and the sample adopts a Q_{II}^{D} phase of typical dimensions expected for an excess water phase formed from Rylo, this seems unlikely.

S7: Radial profiles for L_{II}/Q_{II}^{G} coexistence

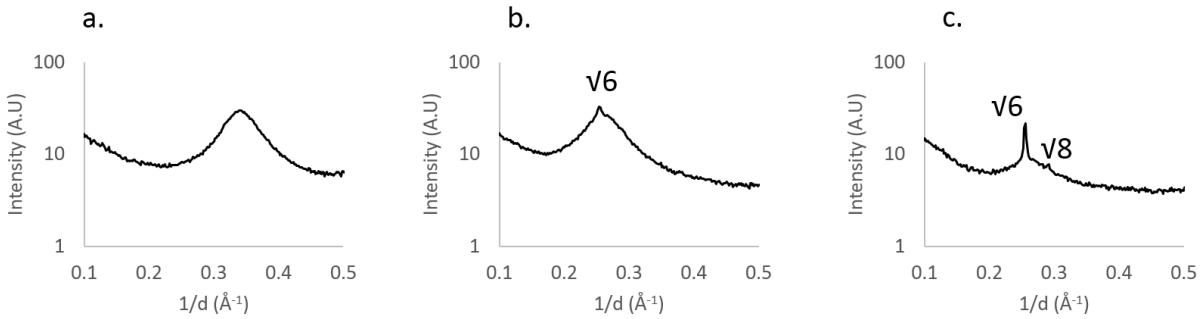

Figure S7. Radial profiles of phytantriol/glycerol films shown in figure 3 with characteristic Bragg peaks noted. (a) Phytantriol and 5% w/w glycerol at RH = 54.2% showing a broad peak characteristic of an L_{II} phase. (b) Phytantriol with 20% w/w glycerol RH = 45% where a coexistence of L_{II} and Q_{II}^{G} phases was observed without the presence of a L_{α}. (c) Phytantriol with 20% w/w glycerol at RH = 34% showing Q_{II}^{G} phase.

S8: Hydrating/Dehydrating measurements

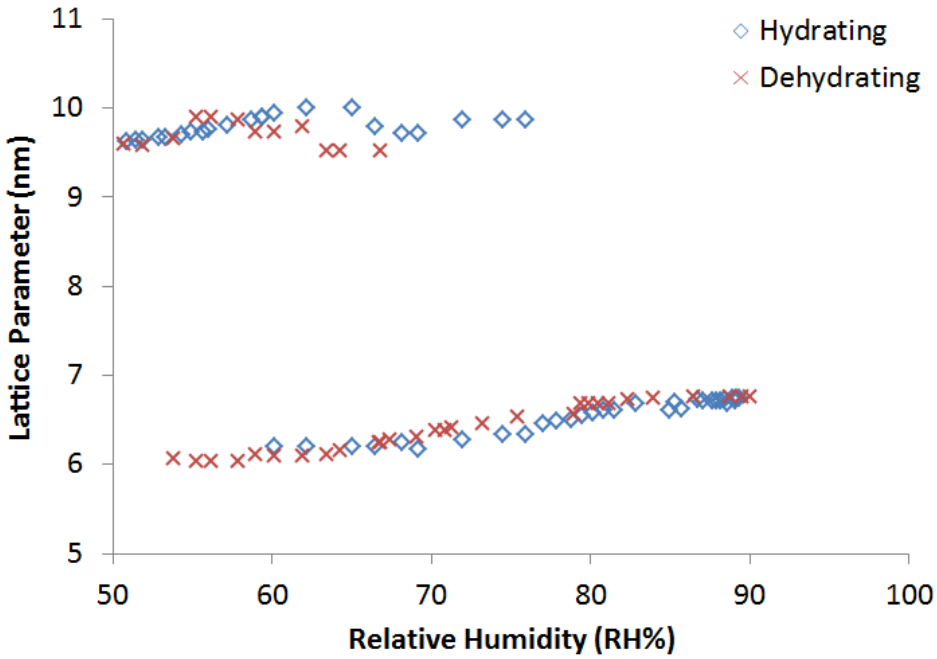

Figure S8. Lattice parameter values for a sample of phytantriol and 20% glycerol under increasing and then decreasing levels of humidity. Values between 9-10nm are for the Q_{II}^{G} phase and those between 6-7 nm are for the Q_{II}^{D} phase.

S9: PEG 6000 induced osmotic pressure measurements upon phytantriol films.

Measurements of PEG 6000 induced osmotic pressure upon thin films of phytantriol were performed by Slaughter[8]. The inside of glass capillaries (1.5 mm radius) was coated in a thin film of phytantriol and filled with a water/PEG 6000 solution. Films were applied to the capillary by a 1mm glass needle coated in phytantriol. Once coated and filled with PEG solution, capillaries were left for several hours to allow sufficient time for the sample to equilibrate before characterization by small-angle X-ray scattering.

Table S9. Mesophase observed in phytantriol/PEG 6000 samples measured in excess water conditions. Taken from work by Slaughter[8].

Grams of PEG per gram of solution (g)	Phase Observed
0.00	Diamond
0.05	Diamond
0.11	Gyroid
0.18	Gyroid
0.25	Gyroid
0.33	Gyroid
0.43	Gyroid/ Lamellar
0.67	Lamellar

S10: Humidity Phase Boundary Predictions

The phase boundaries for the phytantriol/glycerol/water vapor system were predicted by modelling the energetics as follows. For the system to be in equilibrium it is assumed that the chemical potential of the water inside the cubic phase (μ_s) plus the contribution to chemical potential from the bending energy of the lipid bilayer (μ_B) must be equal to the chemical potential of the water vapour (μ_V),

$$\mu_v(\mathrm{RH}) = \mu_B + \mu_s(x)$$

where μ_v varies with RH and μ_s varies with the mole fraction of water to glycerol inside the cubic phase, x. The bending energy of the lipid is assumed to be constant at phase transition because the lattice parameters at phase boundaries are consistent.

Measurements of PEG 6000 induced osmotic pressure on the cubic phase of phytantriol by Slaughter, shown in table S2[8], were used to estimate the bending energy at the Q_{II}^D/Q_{II}^G and Q_{II}^G/L_α transitions. The amount of PEG 6000 required to cause phase transitions were equated to osmotic pressures, P (Pa), using the equation[9],

$$\mathrm{P} = -1.31 \times 10^5 \mathrm{TG}^2 + 141.8 \times 10^{56} \mathrm{G}^2 + 4.05 \times 10^5 \mathrm{G}$$

where G is grams of PEG 6000 per gram of water and T is the temperature (°C). The potential bending energy of the bilayer was then found by,

$$\mu_B = PV_w$$

where V_W is the molar volume of water (1.8×10^{-5} m^3). For the L_{II}/L_α transition the bending energy was estimated from data on humidified films without glycerol,

$$\mu_B = \mathrm{RT} \ln\left(\frac{\mathrm{RH}\%}{100}\right)$$

where R is the gas constant and T is the temperature in Kelvin. RH% is the relative humidity that the lamellar phase was observed to form in our measurements of a pure phytantriol film; in this system we assume the bending energy must equate to the chemical potential of water vapor. The chemical potential of water inside the cubic phase at phase transition (μ_w) varied with the mole fraction of water to glycerol in the cubic phase. The phytantriol/glycerol ratio is set for each sample, however the fraction of glycerol to water vary as humidity increases as the cubic phase takes on water. In order to calculate the amount of moles of water inside the cubic phase at phase transition, the percent with respect to weight of lipid to (water/glycerol) solution at phase transitions, (w/w%$_s$) was taken from measurements by Barauskus et al.[10], which was used to calculate the weight of lipid at phase transition,

$$m_s = \left(\frac{m_l}{100 - \%w/w_s}\right)(\%w/w_s)$$

where m_s is the weight of solution at phase transition and m_l is the weight of the lipid. The total volume of water inside the cubic phase, V_w, was found by

$$V_w = V_s - V_G$$

Where V_s is the total volume of the solution at the phase transition (found from m_s) and V_g is the volume of glycerol. The mole fraction of water inside the cubic phase was then calculated by,

$$x = \frac{\left(\frac{m_s - m_g}{M_w}\right)}{\left(\frac{m_s - m_g}{M_w}\right) + \left(\frac{m_g}{M_w}\right)}$$

Where m_s is the weight of the solution at phase transition, m_g is the weight of glycerol, M_W is the molar weight of water and M_g is the molar weight of glycerol. This was used to estimate μ_W using $\mu_W = RT \ln x$. Finally the phase boundaries were calculated by,

$$RH\% = 100 \exp\left(\frac{\mu_V}{RT}\right)$$

where μ_v is the sum of μ_w and μ_B.

References

1 C. V. Kulkarni, W. Wachter, G. Iglesias-Salto, S. Engelskirchen and S. Ahualli, *Phys. Chem. Chem. Phys.*, 2011, **13**, 3004.
2 S. J. Richardson, P. A. Staniec, G. E. Newby, N. J. Terrill, J. M. Elliott, A. M. Squires and W. T. Górdź, *Langmuir*, 2014, **30**, 13510–13515.
3 T. Snow, M. Rittman and A. Squires, *YAX*, cunninglemon.com
4 ELLIPSHEET: Spreadsheet Ellipsometry, E. Kondoh, 2001, http://www.ccn.yamanashi.ac.jp/~kondoh/ellips_e.html
5 L. F. Hoyt, *Ind. Eng. Chem.*, 1934, **26**, 329–332.
6. Phytantriol basic information, http://www.chemicalbook.com/ProductChemicalPropertiesCB2141592_EN.htm
7 M. A. Green and M. J. Keevers, *Prog. Photovolt. Res. Appl.*, 1995, **3**, 189–192.
8 A. Slaughter, University of Reading, Masters Thesis 2013.
9 H. Chung and M. Caffrey, *Nature*, 1994, **368**, 224–226.
10 J. Barauskas and T. Landh, *Langmuir*, 2003, **19**, 9562–9565.